Optical Constants of Liquid and Solid Methane

John Martonchik and Glenn Orton

Jet Propulsion Laboratory, California Institute of Technology

4800 Oak Grove Drive

Pasadena, CA 91109

to be submitted to Applied Optics

Abstract

The optical constants, n_r+in_i, of liquid methane and phase I solid methane were determined over the entire spectral range using various data sources published in the literature. Kramers-Kronig analyses were performed on the absorption spectra of liquid methane at the boiling point (111 K) and melting point (90 K) and the absorption spectra of phase I solid methane at the melting point and 30 K. Measurements of the static dielectric constant at these temperatures and refractive indices determined over limited spectral ranges were used as constraints in the analyses. Applications of methane optical properties to studies of outer solar system bodies are described

Introduction

Methane in the gas phase has been observed in the atmospheres of the outer planets as well as some of their larger satellites. It is anticipated that methane in both the liquid phase and solid phase also is present in the outer planets and satellites, either as a cloud layer or aerosol haze in the upper atmosphere, or as precipitation. When the results of theoretical modelling of such atmospheres are compared to spectral radiance observations taken either from Earth or spacecraft, information about the radiative structure and chemistry of the atmosphere can be deduced. It is important, however, that the modelling procedure has available the necessary input parameters to accurately perform the required calculations. In particular, in order to calculate the radiative effects of liquid and solid methane in planetary atmospheres, the corresponding optical constants, i.e. the refractive index n_r and the absorption index n_i, must be known as a function of wavelength.

At atmospheric pressure liquid methane exists near the triple point and thus has a limited temperature range, extending from about 90 K to 111 K. Solid methane is known to exist in three phases for pressures below 1 kbar but the thermodynamic conditions encountered in the atmospheres of the outer planets are such that only phase I solid methane (temperature > 20 K at atmospheric pressure) will be present. This form has a face-centered-cubic structure and therefore does not exhibit birefringence.

The results of a literature search for quantitative spectral information on the optical properties of methane in its condensed phases are presented. The data are then analyzed by means of the Kramers-Kronig dispersion relation and the resulting optical constants, n_r+in_i, of the liquid and the phase I solid are displayed in tabular form.

Spectrum Features

Both the liquid phase and the solid phase I of methane have similar absorption spectra. The low frequency end of the spectrum is characterized by a smooth, broad rotational-translational band centered at about 175 cm-l and extending out to about 400 cm-l. At higher frequencies, three strong, sharp fundamental vibrational bands are evident, ν_4 at 1300 cm-l, ν_1 at 2820 cm-', and ν_3 at 3010 cm-l. In the solid phase combinations of fundamental and lattice vibrations also appear at 1350 and 3060 cm-'. At the near infrared and visible frequencies the liquid phase spectrum is characterized by many weak vibrational overtone bands, correlating well with the corresponding gas absorption but shifted toward the lower frequencies by 35-50 cm^{-1} and generally wider in nature 1 In the far ultraviolet a strong absorption continuum appears at about 74,000 cm-' (135 nm) due to photon excitation, photodissociation, photoionization, etc.

Condensed Methane Absorption Data Sources

A. Liquid Phase.

Savoie and Fourier [2] obtained a far-infrared transmission spectrum of a 2 mm sample of liquid methane at 98 K in a study of lattice symmetry of tetrahedral molecules. The data were recorded at a spectral resolution of 1 cm-l and covered the region 20-200 cm-l.

Arning et al.[3] obtained far-infrared spectra of liquid alkanes, including methane at 100 K, in a study of relaxation times and molecular motion. The data are graphically displayed as Lambert absorption coefficients covering the frequent y range 15-275 cm^{-1}.

Weiss et al.[4] show a transmission spectrum of methane at 100 K, covering the frequency range 200-500 cm^{-1}. The spectral resolution was 1.5-2 cm-' and the sample had a thickness of 2.5 mm. This was part of a study of the infrared octupole-induced spectrum of methane gas at room temperature.

Pinkley et al.[5] obtained spectral reflectance measurements of methane at 98 K covering the frequency range 400-4000 cm-'. Results are presented as optical constants in both graphical and tabular form.

Ramaprasad et al.[6] present transmission spectra recorded on photographic plates of a 3 cm thick liquid methane sample at 91-99 K. The data include the bands in the frequency range 5155-16155 cm-l (619-1940 rim).

Patel et al. [1] show an uncalibrated absorption spectrum of liquid methane at 94 K, obtained

using an opto-acoustic technique and covering (he frequent y range 13,300-18,100 cm-l (550-750 rim).

B. Solid Phase

Savoie and Fournier[2] obtained a far-infrared transmission spectrum of solid CH_4 at 77 K (phaseI) for the same instrumental conditions as liquid methane. Also obtained was a spectrum of a solid sample in phase II at 12 K.

Obriot et al. 'presented a transmission spectrum of a 2 mm thick CH_4 sample at 30 K (phase I), covering a frequency range 30-250 cm^{-1}. This was part of a study of solid methane under high pressure.

Fink and Sill [8] obtained spectra of methane at 52 K (phase I) as part of a study of the absorption properties of condensed volatiles in the outer solar system. An interferometer was used, covering the frequency range 1200-4000 cm-l and having a resolution better than 1 cm-l. A variety of different sample thicknesses were used, all in the micrometer range, and the results tabulated as absorption coefficients.

Roux et al. [9] obtained transmission spectra of methane at 20 K (probably phase I) in an investigation to assess the degradation of cryogenically cooled optical surfaces contaminated by condensed gases. They used an interferometer at 4 cm-l resolution covering the frequency range 500-3700 cm^{-1}. Data were collected for 24 sample thicknesses ranging from 0.242 to 11.35 μm and the results tabulated as optical constants.

Khare et al. 10 and Pearl et al. [11] made transmission measurements for a number of thin film samples (thicknesses between 1.2 and 215 μm) of phase I and phase 11 methane at 30 K and 10 K respectively in an ongoing study of optical properties of materials of planetary interest. Khare et al. listed absorption indices for phase I methane between 3800 and 9000 cm-l (1.12 -2.63 μm) and Pearl et al. determined optical constants for both phase I and phase H methane between 1200 and 9000 cm^{-1}.

Dressier and Schnepp[12] obtained ultraviolet transmission spectra of methane at 4.2 K (phase II or possibly phase 111) during a study of intermolecular interactions in hydride molecules. The spectra cover the frequency range 70,000-86,000 cm-' (110 -130 nm) and were obtained for a variety of film thicknesses between 0.01 and 30 pm. The data were displayed graphically as molar absorption coefficients.

In addition to these absorption data, measurements of the static dielectric constant and related parameters were made by Costantino and Daniels 13 for solid methane at a variety of pressures and temperatures. Amey and Cole 14 also measured the dielectric constant for both liquid and solid methane near the melting point and for liquid methane at the boiling point. These data are useful in constraining the refractive index spectrum, derived from the absorption data using a Kramers-Kronig analysis, as described below.

Analysis.

The Kramers-Kronig dispersion relation can be written as

$$n_r(\sigma) = 1 + \frac{2}{\pi} P \int_0^{\infty} \frac{n_i(\sigma')\, \sigma' d\sigma'}{\sigma'^2 - \sigma^2} \qquad (1)$$

where $n_r(\sigma)$ is the refractive index at frequency σ, $n_i(\sigma)$ is the absorption index at σ, and P implies the Cauchy principal part of the integral. The absorption index, in turn, can be obtained from the transmission $T(\sigma)$ through a sample of thickness d,

$$T(\sigma) = \exp[-a(\sigma)\, d], \qquad (2)$$

where $a(\sigma) = 4 \pi \sigma n_i(\sigma)$ is the absorption coefficient at σ. In an application of Eq. (l), Martonchik et al.[16] determined the index of refraction of ammonia ice from the ultraviolet to the far-infrared by using the spectral absorption data found in the literature. If information about the absorption index spectrum is missing in regions where significant absorption occurs, direct application of Eq. (1) can result in an underestimate of $n_r(\sigma)$ at most frequencies. The absorption data for both solid and liquid methane is fairly complete, except in the wavelength region shortward of the blue. Therefore it is desirable to have some knowledge of the refractive index at one or more frequencies to serve as constraints on the integration process described by Eq. (1).

For non-polar molecules, the refractive index at zero frequency, $n_r(0)$, is directly related to the static dielectric constant ε_s by the Maxwell relation $\varepsilon_s = n_r(0)^2$. Amey and Cole[14] measured the static dielectric constant of liquid methane near the melting point (90 K) and boiling point (111 K). The resulting refractive index $n_r(0)$ is 1.293 and 1.274, respectively, with an uncertainty of about 0.0005. For temperatures between the melting and boiling points, Amey and Cole found that the corresponding $n_r(0)$ could be accurately determined by linear interpolation.

Additional liquid methane refractive indices in the visible region of the spectrum were determined by Arakawa et al. 17 using an ellipsometric technique in a study of optical properties of

materials of planetary interest. For a temperature of about 111 K, they obtained a number of n_r values between wavelengths 0.4 and 2.0 μm, ranging from 1.278 at 2.0 μm to 1.286 at 0,4 μm with a listed uncertainty of about 0.005.

The Costantino and Daniels[13] expression for ε_s of solid methane, based on laboratory experiments, depends both on density and temperature. Although their results were obtained for pressures greater than 3 kbar and temperatures ranging from 70 K to 240 K, extrapolation to a pressure of 1 bar produced results in excellent agreement with the measurements of Amey and Cole 14, the only other source of ε_s data known to us. Amey and Cole measured the static dielectric constant of solid methane near the melting point (90 K), implying a value of $n_r(0)$ equal to 1.319 +/- 0.0005; the extrapolated value deduced from the Costantino and Daniels data is 1.320 +/- 0.003, assuming a density of 0.492 gm cm^{-3}. The Costantino and Daniels data also show a linear relationship between ε_s and temperature for a given pressure, with the slope independent of pressure. Assuming that this relationship is also valid at 1 bar, we can infer that $n_r(0)$ at 70 K is 1.320 +/- 0.0005. Extrapolating the temperature down to 20 K implies that $n_r(0)$ is 1.322 +/- 0.001 with a corresponding density of 0.493 +/- 0.010 gm cm^{-3}. Measurements[15], however, near this temperature indicate a density greater than 0.52 gm cm^{-3}, which if true, would appear to invalidate the extrapolation procedure to temperatures this low.

Another refractive index determination for solid methane was made by Roux et al.[9] at a frequency of 15,803 cm-l (633 nm) and a sample temperature of 20 K but their value of 1.35 +/- 0.03 does not have an accuracy as high as the refractive index value at zero frequency. Roux et al. also deduced that the density of their sample was 0.426 gm cm^{-3} which is significantly lower than 0.52-0.53 gm cm^{-3} at 20 K found by other investigators[5]. This may imply that the Roux et al. sample, a thin film deposition, is not representative of bulk solid methane.

A. Absorption index spectrum of liquid methane.

1. 0-500 cm-l spectral region.

The absorption indices obtained from the spectral data of Savoie and Fournier[2] (SF), Arning et al. [3](ATD), and Weiss et al. [4](WLC) are shown in Fig. 1, illustrating considerable differences between the three data sets. Both, the SF and WLC sets were originally expressed in terms of transmission and no quantitative analysis was directly performed on the spectra in either publication. Thus, apparently no effort was made to correct the measured transmissions for any residual cell window effects in order to obtain accurate absorption indices. The ATD data,

however, were originally presented as absorption coefficients and the spectrum subsequently analyzed to determine a correlation function. We therefore believe that the ATD data set is more accurate than the other two and only it was considered in the spectral range 0-300 cm^{-1}. For frequencies higher than 300 cm^{-1} the spectral trend illustrated in the WLC data was assumed and the results scaled to the ATD value at 300 cm-', In our analysis we estimated the uncertainty to be 10% for the value of the absorption indices at frequencies below 300 cm^{-1}, and 20% at frequencies greater than 300 cm-*.

2. 500-4000 cm^{-1} spectral region.

The only liquid methane spectral data known to us in this region is that of Pinkley et al.[5] (PSW). Their results for the absorption index are shown in Fig.2. It is seen that considerable background absorption exist in the data in addition to the fundamental vibration-rotation bands centered at 1300 and 3000 cm 1. This background absorption is considerably larger than their quoted uncertainties but its possible origin was not discussed. Since comparable absorption are not found in either the gas or solid phase spectrum, we feel that it is not real and is probably an artifact of the reflectance data analysis. Therefore, we arbitrarily limited the absorption to the region between 1200 and 1350 cm-l, containing the V_4 transition and also to the region between 2850 and 3120 cm-l, containing the V_1 and V_3 transitions. This latter region in the PSW data is structurally unresolved compared to the same region in the solid phase spectrum and may be due to gaseous methane contamination of the reflectance measurements. We have not done any further reanalysis of the PSW data and have used the absorption indices as published except for the modifications described above. We feel, however, that this spectral region should be studied further in order to verify these results. An estimated uncertainty of 25% in the value of the absorption indices was assumed in the subsequent analysis.

3. 5000-18,100 cm-l spectral region.

There are only very weak absorption features in this part of the methane spectrum but Ramaprasad et al.[6] (RCM) and Patel et al. [1] (PNK) have managed to obtain absorption data with spectral coverage of the two data sets overlapping near 13700 cm-'. The resulting absorption indices are illustrated in Fig. 3. Since the PNK opto-acoustic data are only relative measurements of absorption it was scaled to the RCM data at 13700 cm^{1}, the strongest absorption feature common to both data sets. The PNK data also are of higher quality than the RCM data and in the region of overlap was preferentially used in our analysis. The uncertainty in the resulting

absorption indices was estimated to be 25%.

4, Frequencies greater than 18100 cm-l.

We could find no absorption measurements of liquid methane in this spectral region but there does exist some data on the gaseous phase. Khare et al.[10] has shown that in the red and near-infrared part of the spectrum the absorption indices of gaseous methane at low resolution are very similar to the those for the liquid phase, provided the gas density is raised to that of the liquid. A similar conclusion was reached by Pinkley et al.[5] for the fundamental bands. Therefore, we present the gaseous data in this spectral range in order to complete our study of the characteristic features of the methane spectrum and also to use these data, appropriately scaled to the density of the liquid state, in our determination of spectral refractive indices.

A review of all the absorption cross section measurements of methane gas from 2 to 160 nm (62500 to 500000 cm^{-1}) was completed by Hudson[18] in 1971; since then, additional measurements in the wavelength range 140 to 160 nm were made by Mount et al.[19]. Assuming a gas density at STP of 7. 15x 10^{-4} gm cm^{3},he resulting absorption indices are illustrated in Fig. 4. Also shown are the scaled absorption indices for the liquid phase, assuming a liquid methane density of 0.424 g cm^{-3} (111 K). It is expected that the uncertainty in the indices will be large; we have assumed 50% for any given frequency. But it should be noted that the frequency-integrated absorption index is more tightly constrained since this spectral region dominates the integral described by Eq. (1) and the refractive index at zero frequency is well known.

B. Optical Constants of Liquid Methane.

Use of the Kramers-Kronig relation in Eq. (1) with the absorption indices described above produced a refractive index spectrum at the boiling point (111 K) which was close to, but consistently below, the measured indices of Arakawa et al. [17] and the value at zero frequency inferred from the static dielectric constant. A sample of the measured values of n_r and the corresponding computed values are listed in Table 1, showing a difference maximum of about 0.018 at 1.0 and 2.0 μm and a difference minimum of 0.006 at zero frequency. Since the general level of the refractive indices throughout the spectrum is determined mainly by the absorption shortward of the ultraviolet wavelengths, this reasonably good agreement indicates that the scaled gaseous absorption values used in this spectral region are probably a fair representation of the actual liquid methane spectrum.

In an effort to produce a better match between computations and measurements, the

gaseous absorption values were subsequently resealed by small amounts. An adjustment to this particular part of the liquid methane absorption spectrum is reasonable since the original scaling factor, defined by the liquid density to gas density ratio, can only be considered an approximation. The results, also shown in Table 1, are for the two cases when the absorption indices in Fig. 4 were increased by 2.5% and 5.7%. The smaller increase of 2.5% produces a refractive index at zero frequency, $n_r(0)$, which agrees with the static dielectric constant measured by Amey and Cole[14] but also produces indices in the visible and near-IR which are consistently below the measurements of Arakawa et al. by about 0.011. The larger scaling increase of 5.7% does result in refractive indices in good agreement with the Arakawa et al. values (all are within the 0.005 uncertainty) but now overshoots $n_r(0)$ by 0.008. Other regions of the absorption spectrum are not strong enough for any reasonable resizing of their values (within the allowable uncertainty limits) to significantly change the results in Table 1. For instance the collision-induced absorption region in the far infrared (Fig. 1) or the strongly absorbing fundamental bands between 1200 and 3100 cm^{-1} can be scaled down by 50% and $n_r(0)$ is reduced by only 0.001 and 0.002 respectively. If we assume that the refractive indices of Arakawa et al. are correct then the corresponding result of 1.282 for $n_r(0)$ implies a static dielectric of 1.644. This is larger than the value of 1.623 measured by Amey and Cole (and outside the uncertainty of 0.0005) and appears inconsistent with $n_r(0)$ determined at other temperatures as discussed later.

Table 2 lists both refractive and absorption indices of liquid methane at both 111 K and 90 K for selected frequencies. Those optical constants followed by a positive or negative sign indicate a local maximum or minimum respectively. The refractive indices at 111 K were computed assuming that $n_r(0)$ is 1.274, implying a resealing of the far UV absorption spectra in Fig. 4 by 2.5%, and that the rest of the absorption indices n_i are as indicated in Figs. 1 through 3. Using the static dielectric constant at 90 K of 1.672, as determined by Amey and Cole[14], a value of 1.293 was assumed for $n_r(0)$ at the melting point. The n_i at 90 K were determined by simply scaling the n_i at 111 K by the ratio of the methane densities at these two temperatures. Since the uncertainties in the absorption indices are much larger than this first-order temperature correction, this temperature correction of n_i serves only to indicate the magnitude of the temperature dependence. The far UV absorption indices then were scaled up by an additional 2.5% to achieve the assumed value of $n_r(0)$.

The region with frequencies greater than 60,000 cm^{-1} (167 nm) is also included in the table. Caution must be used, however, in regards to the optical constants listed for this spectral

region since they are based on an extrapolation from the gaseous phase. We believe, nevertheless, that these values represent a reasonable approximation to the actual optical constants.

C. Absorption index spectrum of solid methane.

1. 0-500 cm^{-1} spectral region.

The two data sets in this spectral region are those of Obriot et al.[7] (OFMVK) and Savoie and Foumier [2] (SF). Since the data for both sets are spectral transmission, transformation to absorption indices according to Eq. (2) will include some residual cell window effects which cannot be adequately accounted for due to insufficient information. Given this limitation, the resulting absorption indices are illustrated in Fig. 5. There is some difference between the two sets of which a large part may be due to the fact that the OFMVK data were taken at 30 K (absorption peak at 120 cm^{-1}) and the SF data at 77 K (absorption peak at 170 cm^{-1}). We assume that this difference is real and use both data sets in the optical constants analysis. At frequencies between 200 and 500 cm-l, no ice data is available so we used the corresponding liquid methane absorption indices of Aming et al.[3] and Weiss et al.[4], scaled to the OFMVK and SF data. This extrapolation is also shown in Fig. 5. The absorption index uncertainty was estimated to be 15% for values shortward of 200 cm^{-1} and 25% for those extrapolated values between 200 and 500 cm-l.

2. 500-4000 cm-' spectral region.

The three absorption index data sets available in this spectral region are those of Fink and Sill [8] (FS), Roux et al.[9] (RWSP), and Pearl et al.[11] (PNOK) and all are shown in Fig. 6. The numerical values of the FS absorption coefficients were supplied by Fink (personal communication). This data set at 52 K certainly pertains to phase I; the RWSP data set at approximately 20 K may pertain to phase 11, The FS coefficients, however, was not corrected for variable interface reflection effects within the cell. Thus, in the region of strong sample absorption where the refractive index is varying, simply using Eq. (2) to determine the absorption coefficient, as Fink and Sill have done, will result in some error. The data of RWSP, on the other hand, were analyzed with all of the cell effects taken into account and the results displayed as optical constants. The absorption coefficient values of the PNOK data, supplied by Pearl (personal communication), are the result of an analysis similar to that of Roux et al.. The three absorption index spectra show general agreement with each other in the regions of strong absorption. Some differences between the spectra can be attributed to the incomplete analysis of the FS data as

described above and possibly to the different temperatures of the methane samples. At frequencies between 2300 and 3700 cm-', however, the RWSP data show a substantial absorption continuum, in contrast to the FS and PNOK data. Another such region is evident between 700 and 900 cm^{-1}. It is not clear what the nature of this absorption might be, or if it is an artifact of the analysis process. There are indications of contamination by trace constituents in the RWSP data, with at least one sharp absorption feature probably due to $C0_2$ showing up at 2340 cm-'. In the FS spectrum there is also an unidentified feature at 3700 cm^{-1} which may also be due to some contaminant. In view of the differences between the various data sets, we have selected the PNOK data in our analysis because it appears to be free of the unexplainable features which seem to plague the other two data sets, particularly that of Roux et al., and also because of the rigorous analysis the transmission data underwent to account for sample cell optical effects, unlike that of the FS data. Pearl et al. estimated the absorption index uncertainty to be about 15% in this spectral region.

3. 4000-9000 cm-' spectral region.

The absorption indices of Pearl et al.[11] measured at 30 K were used in this spectral region. and are shown in Fig. 7. The results should be quite good since substrate optical effects were accounted for in their analysis. Pearl et al. estimated the uncertainties in these absorption indices to be about 20%.

4. Frequencies greater than 9000 cm-*.

The only data in this region are that of Dressier and Schnepp *[2], starting at 72,000 cm^{-1} (140 nm) and taken at a temperature of 4.2 K. These data show that the far ultraviolet absorption is blue-shifted about 5 nm from that of the gaseous phase. This corresponds to about a 2500 cm^{-1} shift towards higher frequencies, which is considerably larger than the shifts observed throughout the rest of the spectrum. Comparing the gas and liquid phases, for example, the observed shift of the liquid absorption peaks in the visible and near infrared is about 50 cm^{-1} toward lower frequencies. From the data reviewed in this paper, the observed absorption peak shifts between the liquid and the phase I solid states are also considerably less than 50 cm-'. Therefore, the Dressier and Schnepp data, corresponding to solid phase III, is probably not indicative of the absorption characteristics of phase I. Considerable variation in the absorption spectrum between phase I and phases II or III also occurs in the far-infrared region[2,3]. We have, therefore, assumed in our analysis that the phase I solid state for methane has an absorption spectrum shortward of

167 nm which is more similar to the liquid or gaseous state than to the phase II or 111 solid state and as such we have again used the gaseous absorption data, now scaled to the density of the phase I solid state at the melting point. At a melting point temperature of 90 K the density is assumed to be 0.492 gm cm^{-3} (see Costantino and Daniels[12]). The estimated uncertainties in the absorption indices are the same as for liquid methane, about 50%.

D. Optical Constants of Solid Methane.

In an analysis similar to that for liquid methane, the Kramers-Kronig relation, expressed by Eq. 1, was used to obtain the refractive index spectra of phase I solid methane at the melting point (90 K) and at 30 K. Since much of the original absorption index spectra described above was obtained at temperatures near 30 K, these n_i displayed in Figs. 4 through 7 were assumed to represent the absorption spectrum of methane at 30 K. Using the same temperature-dependence correction scheme as for liquid methane, namely scaling the absorption spectrum by the ratio of the densities at the two temperatures, the n_i at 90 K also was evaluated. Again, owing to the large uncertainties in the absorption spectrum at 30 K, this correction procedure indicates only the magnitude of the temperature dependence. The Kramers-Kronig analysis using this 90 K spectrum resulted in a value for $n_r(0)$ of 1.310, smaller than the values of 1.319 and 1.320 implied from the static dielectric constants determined by Amey and Cole[14] and Costantino and Daniels[13] respectively. By allowing the scaling of the far UV part of the absorption spectrum to be adjusted upwards by 2.9%, however, the computed $n_r(0)$ could be brought into agreement with the noted static dielectric constant measurements.

Pearl et all [1] also determined refractive indices between 1200 and 4500 cm^{-1} for phase I solid methane at 30 K. Resealing the original 30 K far UV absorption spectrum upward by 4.0% allows these refractive indices to be matched. resulting in an $n_r(0)$ at 30 K equal to 1.329. It was noted by Pearl et al. that their refractive indices were in good agreement with those derived by Roux et al.[9]

The optical constants of phase I solid methane at 90 K and 30 K are listed in Table 3 for selected frequencies. The positive and negative sign convention has the same meaning as in Table 2. More complete versions of Tables 2 and 3 can be obtained from the authors.

Discussion

We have used a variety of data sources to obtain a complete spectrum of the optical constants for both liquid and phase I solid methane. Although the absorption data in certain

spectral regions from multiple sources showed some significant differences, there appears to be no major problems in the relation of refractive index n_r to absorption index n_i via the Kramer-Kronig expression. More explicitly, the computed values of n_r, via the Kramer-Kronig expression, are in reasonably good agreement with the experimentally determined values.

There is, however, a troubling inconsistency between the value of $n_r(0)$ for liquid methane at the boiling point (111 K) as determined by Amey and Cole[14] and the values of n_r at visible wavelengths as determined by Arakawa et al.[17]. Recall that Amey and Cole obtained a value for the static dielectric constant ε_s of 1.623 equivalent to $n_r(0)$ equal to 1.274. But this value could not be fit simultaneously in the Kramers-Kronig analysis with the Arakawa et al. refractive index values for any reasonable adjustments to the far UV region absorption coefficients. The Amey and Cole value of ε_s, however, is consistent with an essentially constant Clausius-Mossotti (CM) function,

$$CM = \frac{\varepsilon_s - 1}{\varepsilon_s + 2} \frac{M}{\rho} \tag{3}$$

evaluated in Table 4 for the liquid phase at 111 K (boiling point), the liquid and the solid phase at 90 K (melting point) and for the solid phase at 30 K. Here M is the molecular weight equal to 16.05 and p is the density in gm cm^{-3}. The density at 30 K, 0.502 gm cm^{-3}, was determined by extrapolating the temperature and density dependent empirical function for ε_s of Costantino and Daniels[13] down to 30 K and using the value for ε_s of 1.766 ($n_r(0)$ = 1.329) obtained from fitting the refractive indices of Pearl et al.[11] as described earlier. Now, if $n_r(0)$ of liquid methane at the boiling point is assumed to be 1.282, the value obtained by fitting the refractive indices of Arakawa et al., then ε_s is 1.644 and the value of the CM function becomes 6.69 which is considerably larger than the values of the CM function for the other temperatures in Table 4.

For this reason $n_r(0)$ equal to 1.274 is considered to be a more accurate value than 1.282 and therefore it was used in the Kramers-Kronig analysis of the 111 K absorption spectrum, the results of which are displayed in Table 2. Using this lower value for $n_r(0)$, the computed n_r at visible wavelengths are about 0.01 lower than those determined by Arakawa et al. implying that some systematic error may have entered into their measurements. The trend of the refractive indices of Arakawa et al. also deviates somewhat from that of the Kramers-Kronig analysis in that those indices in the blue region of the spectrum around 25,000 cm^{-1} exhibit less of an increase with frequency than expected, considering the strong far UV absorption upturn near 70,000 cm-'.

It is possible to better fit the measured trend but it would require that the peak absorption near 110,000 cm^{-1} (see Fig. 4) be shifted to much higher frequencies (to about 150,000 cm-1) and the total absorption be substantially increased (by about 75%). Such a distortion of the far UV absorption spectrum seems unwarranted.

An estimate of the uncertainty in the refractive indices displayed in Tables 2 and 3 was determined by using the absorption indices at the limit of their estimated uncertainties and the subtractive form of Eq. (1), which allows the refractive index at a frequent y σ_0 to be fixed. This modified form of Eq(1) can be written as

$$n_r(\sigma) = n_r(\sigma_0) + \frac{2}{\pi}(\sigma^2 - \sigma_0^2)\, P\int_0^\infty \frac{n_i(\sigma')\,\sigma'\,d\sigma'}{(\sigma'^2 - \sigma^2)(\sigma'^2 - \sigma_0^2)} \quad (4)$$

Setting σ_0 at zero frequency, the computed n_r uncertainty estimates for both liquid and solid methane are less than 0.002 in those regions of the spectrum where absorption is at a minimum. The two strongly absorbing regions around 1300 and 3000 cm^{-1}, however, attain uncertainties at the local n_r maxima and minima of 0.022 and 0.011, respectively, for the liquid state and 0.078 and 0.020, respectively, for the solid state. For the far UV region it is difficult to estimate the accuracy of the computed refractive indices. We originally estimated the uncertainty in the absorption coefficients to be about 50?%. The spectrally integrated absorption, however, must be reasonably close to the true condition because of its strong effect on $n_r(0)$ which was able to be matched with only a minimum of adjustment. The actual shape of the far UV absorption can be expected to have some variation from the values listed in Tables 2 and 3 and graphed in Fig. 4. but at most frequencies in this region it is expected that this variation is less than about 20%. This then implies a n_r uncertainty of less than 0.05 at any frequency higher than 60,000 cm-l.

Although there is general agreement among all the various data sets and types, absorption data deficiencies with regard to accuracy are still a problem in various spectral regions. The collision-induced absorption for both the liquid and solid states in the far infrared region around 200 cm-* still is not well characterized, especially for the solid state at frequencies between 200 and 500 cm-l. The liquid state has only the measurements of Pinkley et al.[5] at the fundamental bands near 1300 and 3000 cm-l and these contain relatively prominent background absorption near the absorption peaks. Confirmation of these features would be desirable since the solid state measurements of Pearl et al.[11] in these same spectral regions do not show such features. The seemingly high values for the refractive indices in the visible and near infrared of Arakawa et al.[17]

should also be confirmed by additional measurements. Finally, any absorption data in the far UV for either the liquid or phase I solid state would be extremely useful for validating the assumption of gaseous absorption similarity used in our analyses.

Application

These results have direct application to the study of atmospheres in the outer solar system. Two brief examples follow. In the first, the influence of liquid methane clouds in the atmosphere of Titan, Saturn's largest satellite, has been modelled following the properties suggested by Toon et al. 20. Evidence for such clouds is quite indirect and follows only from the expectation that the amount of CH_4 gas in the lower troposphere near Titan's surface is large enough so that condensation takes place at higher and colder latitudes. The far infrared spectrum of Titan is shown in Fig. 8, illustrating the influence of the 100 μm droplet cloud and sub-μm haze model preferred b y Toon et al.[20] and constrained by Voyager infrared spectrometer data for wavenumbers200 cm^{-}* and greater. The 50 cm^{-}1 emission feature corresponds to the location of maximum N_2-N_2 collision-induced gaseous absorption. The emission feature is centered on a broad absorption region and represents thermal emission from a region where temperature is increasing with altitude (and brightness is increasing with optical thickness), While both the haze and the CH_4 droplet cloud influence Titan's spectrum above 50 cm-l quite strongly, their influence on spectral regions below 50 cm^{-}1 is negligible, even for 100 μm liquid CH_4 droplets. Thus, the spectral region shortward of 50 cm^{-1} is useful for sounding temperatures in Titan's lower atmosphere up through a level just above the temperature minimum with little confusion from known or suspected clouds or hazes.

In the second example solid CH_4 crystals are expected to form in Neptune's troposphere near the 1.5 bar level from a large reservoir of gaseous CH_4 in the deep atmosphere where its mixing ratio is on the order of 1 -2%. A comparison of Voyager infrared and radio occultation measurements indicates that this cloud is optically significant 21. Three spectra, simulating the conditions by which the Conrath et al. [21] spectra were constrained, are shown in Fig. 9. In this illustration all spectra were constrained to the same brightness temperature at 200 cm-l. Cloud bottoms were placed near the expected CH_4 condensation pressure of 1.5 bars and tops near the temperature minimum at 0.2 bar; the cloud particle scale height is 0.15 times the pressure scale height. Fig. 9 shows that observations of the spectrum shortward of the Voyager infrared spectrometer limit of 200 cm^{-}1, as might be obtained by the European Space Agency's Infrared Space Observatory Long Wavelength Spectrometer (LWS) instrument, will distinguish between 3 μm and 30 or 0.3 μm but not between 30 and 0.3 μm particles. This is also true of the faint

continuum near 1000 cm- 1 which might be detected between many stratospheric emission lines in this region (not shown in the figure).

Conclusion

Data on the optical properties of liquid methane and phase I solid methane, obtained by performing a literature search, were collectively analyzed via the Kramers-Kronig relation to determine the spectral optical constants from O to 500,000 cm^{-1}. Much of the data consisted of spectral transmission measurements which then were converted to absorption coefficients. In these cases corrections for sample cell multiple reflection effects were ignored, due mainly to incomplete information concerning the sample cell and also to the quality of the data. For both liquid and phase I solid methane no data could be found on the strong far ultraviolet absorption at frequencies beyond 60,000 cm^{-1} and so the gaseous absorption spectrum in this frequency region was used as a substitute, scaled by the appropriate density ratios. Measured static dielectric constants and refractive indices in limited spectral ranges were used as constraints in the Kramers-Kronig analysis. Further improvements in the accuracy of the optical constants for both the liquid and phase I solid states of methane will require additional measurements particularly in the far UV portion of the spectrum. However, the current status of the optical constants as reviewed in this paper is sufficiently complete to be useful in the study of the bodies of the outer solar system.

Acknowledgments.

We want to thank J. Pearl, U. Fink, and B. Khare for tabular forms of their data and J. Pearl for many helpful comments. This research was carried out by the Jet Propulsion Laboratory, California Institute of Technology, under contract with the National Aeronautics and Space Administration.

Figure Captions

Figure 1. Absorption index spectra of liquid methane (dashed line - SF; dotted line - WCL; crosses - ATD; solid line - best estimate).

Figure 2. Absorption index spectra of liquid methane (dashed line - PSW; solid line - best estimate).

Figure 3. Absorption index spectra of liquid methane (crosses and dashed line - RCM; stars - PNK; solid line - best estimate).

Figure 4. Absorption index spectra of methane (dashed line - liquid phase best estimate; solid line - solid phase best estimate).

Figure 5. Absorption index spectra of solid methane (dashed line - OFMVK; stars - SF; diamonds - extrapolation; solid line - best estimate).

Figure 6. Absorption index spectra of solid methane (dotted line - RWSP; dashed line - FS; stars - PNOK; solid line - best estimate).

Figure 7. Absorption index spectra of solid methane (crosses - PNOK; solid line - best estimate).

Figure 8. Model far infrared spectra of Titan for an emission angle near O“. Clear atmosphere (dashed line) and an atmosphere with a haze and a CH_4 condensate cloud of 100 μm droplets (solid line).

Figure 9. Model infrared spectra of Neptune considering continuum components only. Number density of particles in solid CH_4 cloud is adjusted in each model to obtain same brightness temperature at 200 cm^{-1}. Cloud with 0.3 μm particles (dotted line), 3 μm particles (solidline), 30 μm particles (dashed line).

References.

1. C.K.N. Pate], E. T. Nelson, and R.J. Kerl, "Opto-Acoustic Study of Weak Optical Absorption of Liquid Methane," Nature 286,368 (1980).

2. R. Savoie and R.P. Fournier, "Far-infrared Spectra of Condensed Methane and Methane-d4," Chem. Phys. Letters 7, 1 (1970).

3. H.-J. Arning, K. Tibulski, and Th. Dorfmuller, "Collision-Induced Spectra of Simple Liquids," Ber. Bunsenges. Phys. Chem. 85, 1068 (1981).

4. S. Weiss, G.E. Leroi, and R.H. Cole, "Pressure-Induced Infrared Spectrum of Methane," J. Chem. Phys. 50,2267 (1969).

5. L.W. Pinkley, P.P. Sethna, and D. Williams, "Optical Constants of Liquid Methane in the Infrared," J. Opt. Sot. Am. 68, 186 (1978).

6. K.R. Ramaprasad, J. Caldwell, and D.S. McClure, "The Vibrational Overtone Spectrum of Liquid Methane in the Visible and Near Infrared: Applications to Planetary Studies," Icarus 35, 400 (1978).

7. J. Obriot, F. Fondere, Ph. Marteau, H. Vu and K. Kobashi, "Far- Infrared Spectra of Solid CH4 Under High Pressure," Chem. Phys. Letters 60,90 (1978).

8. U. Fink and G.T. Sill, "The Infrared Spectral Properties of Frozen Volatile," in 'Comets', L.L. Wilkening, Ed. (U. of Arizona Press, Tucson, 1982), pp. 164-202.

9. J.A. Roux, B.E. Wood, A.M. Smith and R.R. Plyler, "Infrared Optical Properties of Thin CO, NO, CH4, HC1, N20, 02, N2, Ar, and Air Cryofilms," Arnold Engineering Development Center Tech. Rep. AEDC- TR-79-81 (1979); NTIS accession number AD A088269.

10. B.N. Khare, W.R. Thompson, C. Sagan, E.T. Arakawa, C. Bruel, J.P. Judish, R.K. Khanna, and J.B. Pollack, "Optical Constants of Solid Methane," NASA CP-3077, First International Conference on Laboratory Research for Planetary Atmospheres, Bowie State Univ., MD, 25-27 October 1989, pp. 327-333.

11. J. Pearl, N. Ngoh, M. Ospina, and R. Khanna, "Optical Constants of Solid Methane and Ethane from 10,000 to 450 cm^{-1}," J. Geophys. Res. 96, 17,477 (1991).

12. K. Dressier and O. Schnepp, "Absorption Spectra of Solid Methane, Ammonia, and Ice in the Vacuum Ultraviolet," J. Chem. Phys. 33,270 (1960).

13. M.S. Costantino and W.B. Daniels, "Dielectric Constant of Compressed Solid Methane at Low Temperature," J. Chem. Phys. 62,764 (1975).

14. R.L. Amey and R.H. Cole, "Dielectric Constants of Liquefied Noble Gases and Methane," J. Chem. Phys. 40, 146 (1964).

15. V.G. Manzhelii and A.M. Tolkachev, "Densities of Ammonia and Methane in the Solid State," Sov. Phys. Solid State 5,2506 (1964).

16. J.V. Martonchik, G.S. Orton, and J.F. Appleby, "Optical Constants of NH3 Ice from the Far Infrared to the Near Ultraviolet," Appl. Opt. 23,541 (1984).

17. E.T. Arakawa, P.D. Clapp, T.A. Calcott, B.N. Khare, and C. Sagan, "Refractive Indices of Liquid Methane and Ethane," Bull. Am. Phys. Sot. 31,700 (1986).

18. R.D. Hudson, "Critical Review of Ultraviolet Photoabsorption Cross Sections for Molecules of Astrophysical and Aeronomic Interest," Rev. Geophys. SpacePhys.9,305(1971).

19. G.H. Mount, E.S. Warden, and H.W. Moos, "Photoabsorption Cross Sections of Methane from 1400 to 1850 A," Astrophys. J. 214, L47, (1977).

20. O.B. Toon, C.P. McKay, R. Courtin, and T.P. Ackerman, "Methane Rain on Titan," Icarus 75, 255 (1988).

21. B.J. Conrath, D. Gautier, G.F. Lindal, R.E. Samuelson, and W.A. Shaffer, "The Helium Abundance of Neptune from Voyager Measurements," J. Geophys. Res. 96, 18907 (1991)..

Table 1. Liquid CH_4 Refractive Indices

Frequency (cm^{-1})	$n_r^{(1)}$	$n_r^{(2)}$	$n_r^{(3)}$	$n_r^{(4)}$	Wavelength (μm)
0	1.274	**1.268**	**1.274**	**1.282**	**00**
5,000	**1.278**	**1.260**	**1.267**	**1.275**	**2.0**
8,333	1.280	1.262	1.268	1.277	1.2
10,000	1.280	1.262	1.269	1.277	1.0
12,500	1.281	1.264	1.270	1.279	0.8
16,667	1.283	1.266	1.273	1.282	0.6
25,000	1.286	1.273	1.281	1.289	**0.4**

[1] $n_r(0)$ determined by Amey and Cole (ref.14); other n_r determined by Arakawa et al. (ref. 17)
[2] computed using original far UV absorption spectra in Fig. 4
[3] computed using original far UV absorption spectra scaled up by 2.5%
[4] computed using original far UV absorption spectra scaled up by 5.7%

Table 2. Optical Constants of Liquid Methane

Frequency (cm-l)	n_r(112 K)	n_i(112 K)	n_r(90 K)	n_i(90 K)	Wavelength (μm)
0.0	1.274	0.000E+00	1.293	5.302E-05	
140.0	1.273	1.353 E-03+	1.291	1.442E-03+	71.43
240.0	1.272-	6.234E-04	1.290-	6.645E-04	41.67
1210.0	1.311+	1.00 1E-02	1.331+	1.067E-02	8.26
1230.0	1.305 -	2.002E-02	1.325-	2.135E-02	8.13
1282.5	1.342+	7.499E-02	1.365+	7.994E-02	7.80
1300.0	1.258	1.600E-01+	1.275	1.706E-01+	7.69
1317.5	1.183-	7.249E-02	1.195-	7.728E-02	7.59
2800.0	1.284+	1.000E-02	1.303+	1.066E-02	3.57
2915.0	1.281-	2.000E-02	1.300-	2.132E-02	3.43
2970.0	1.291+	4.000E-02	1.310+	4.264E-02	3.37
3000.0	1.261	7.000E-02+	1.278	7.462E-02+	3.33
3040.0	1.227-	3.000E-02	1.242-	3.198E-02	3.29
5120.0	1.267	8.393E-07+	1.285	8.947E-07+	1.953
5175.0	1.267	1.476E-06+	1.285	1.574E-06+	1.932
8055.0	1.268	7.903E-08+	1.286	8.425E-08+	1.241
8095.0	1.268	1.573E-07+	1.286	1.677E-07+	1.235
9865.0	1.269	9.438E-07+	1.287	1.006E-06+	1.014
10000.0	1.269	7.799E-07+	1.287	8.313E-07+	1.000
10130.0	1.269	5.892E-07+	1.287	6.281E-07+	0.9872
10265.0	1.269	4.651E-07+	1.287	4.958E-07+	0.9742
11255.0	1.270	1.782E-06+	1.288	1.899E-06+	0.8885
11530.0	1.270	3.106E-O7+	1.288	3.311E-07+	0.8673
11880.0	1.270	4.689E-08+	1.288	4.998E-08+	0.8418
12510.0	1.270	5.725E-08+	1.288	6.103E-08+	0.7994
12740.0	1.271	3.748E-08+	1.289	3.995E-08+	0.7849
13700.0	1.271	9.294E-08+	1.289	9.907E-08+	0.7299
13940.0	1.271	1.085E-07+	1.289	1.156E-07+	0.7174
14170.0	1.271	7.862E-09+	1.289	8.381E-09+	0.7057
14585.0	1.272	2.51OE-O9+	1.290	2.675E-09+	0.6856
14935.0	1.272	4.476E-09+	1.290	4.771E-09+	0.6696
16090.0	1.273	1.830E-07+	1.291	1.951E-07+	0.6215
16715.0	1.273	1.095E-09+	1.291	1.167E-09+	0.5983
17150.0	1.273	1.160E-09+	1.291	1.237E-09+	0.5831
25000.0	1.281	0.000E+00	1.299	0.000E+00	0.4000
74773.0	1.660+	1.702E-01	1.703+	1.814E-01	0.1337
83333.0	1.456	3.128E-01+	1.486	3.336E-01+	0.1200
86051.0	1.442-	3.024E-01	1.471-	3.225E-01	0.1162
91991.2	1.476+	3.527E-01	1.508+	3.761E-01	0.1087
98809. S	1.417-	4.472E-01	1.445-	4.768E-01	0.1012
100000.0	1.420+	4.551E-01	1.448+	4.853E-01	0.1000
111111.0	1.196	6.096E-01+	1.209	6.501E-01+	0.0900
183333.5	0.865-	2.004E-01	0.856-	2.137E-01	0.0545
5000000.0	1.000	O.OOOE+OO	1.000	0.000E+00	0.0020

Table 3. Optical Constants of Solid Methane

Frequency (cm^{-1})	n_r(90 K)	n_i(90 K)	n_r(30 K)	n_i(30 K)	wavelength (μm)
0.0	1.319	0.000E+00	1.329	0.000E+00	
160.0	1.317	2.583 E-03+	1.327	2.636E-03+	62.50
275.0	1.316-	7.472E-04	1.326-	7.624E-04	36.36
1297.0	1.829+	5.086E-01	1.849+	5.190E-01	7.71
1300.0	1.265	9.598E-01+	1.274	9.794E-01+	7.69
1302.8	0.826-	4.988E-01	0.826-	5.090E-01	7.68
2805.0	1.321+	2.570E-03	1.331+	2.622E-03	3.57
2820.0	1.319	4.574E-03+	1.329	4.667E-03+	3.55
2830.0	1.318-	2.877E-03	1.328-	2.936E-03	3.53
3002.5	1.450+	1.063E-01	1.463+	1.085E-01	3.33
3010.0	1.339	2.564E-01+	1.349	2.617E-01+	3.32
3016.5	1.191-	1.432E-01	1.198-	1.461E-01	3.32
4200.0	1.316+	5.547E-03	1.326+	5.660E-03	2.38
4203.0	1.312	9.199E-03+	1.321	9.387E-03+	2.38
4207.5	1.306-	5.058E-03	1.316-	5.161E-03	2.3.8
4293.0	1.314+	3.096E-03	1.323+	3.160E-03	2.33
4303.0	1.311	6.189E-03+	1.320	6.316E-03+	2.32
4315.0	1.307-	3.453E-03	1.317-	3.523E-03	2.32
5567.0	1.311	1.807E-04+	1.321	1.844E-04+	1.796
5602.0	1.311	8.213E-05+	1.321	8.381E-05+	1.785
5802.0	1.311	2.446E-04+	1.321	2.496E-04+	1.724
5993.0	1.311	4.737E-04+	1.321	4.833E-04+	1.669
7082.0	1.312	2.368E-05+	1.322	2.416E-05+	1.412
7131.0	1.312	3.642E-05+	1.322	3.716E-05+	1.402
7220.0	1.312	9.073E-06+	1.322	9.258E-06+	1.385
7294.0	1.312	1.828E-05+	1.322	1.866E-05+	1.371
7483.0	1.312	5.023E-05+	1.322	5.126E-05+	1.336
8587.0	1.313	4.577E-05+	1.322	4.671E-05+	1.165
8784.0	1.313	1.900E-05+	1.323	1.939E-05+	1.138
10000.0	1.313	0.000E+00	1.323	0.000E+00	1.000
25000.0	1.326	0.000E+00	1.336	0.000E+00	0.4000
74773.0	1.768+	1.981E-01	1.791+	2.042E-01	0.1337
83333.0	1.530	3.632E-01+	1.547	3.744E-01+	0.1200
86051.0	1.515-	3.518E-01	1.531-	3.627E-01	0.1162
91991.0	1.554+	4.104E-O1	1.571+	4.231E-01	0.1087
98810.0	1.486-	5.203E-01	1.501-	5.364E-01	0.1012
101316.0	1.491+	5.681E-01	1.506+	5.856E-01	0.0987
111111.0	1.228	7.096E-01+	1.235	7.315E-01+	0.0900
183334.0	0.842-	2.332E-01	0.837-	2.404E-01	0.0545
875000.0	0.994+	2.607E-03	0.993+	2.688E-03	0.0114
5000000.0	0.971	0.000E+00	0.970	0.000E+00	0.0020

Table 4. C1ausius-Mossotti Function for Methane

T (K)	ρ (gm cm^{-3})	ε_s	CM (cm^3 mole^{-1})
111	0.424[1]	1.623[1]	6.51
90 (liquid)	0.452[2]	1.672[1]	6.50
90 (solid)	0.492[2]	1.740[1]	6.45
30	0.502[2]	1.766[3]	6.50

[1] see Amey and Cole (ref. 14)

[2] see Costantino and Daniels (ref. 13)

[3] see text

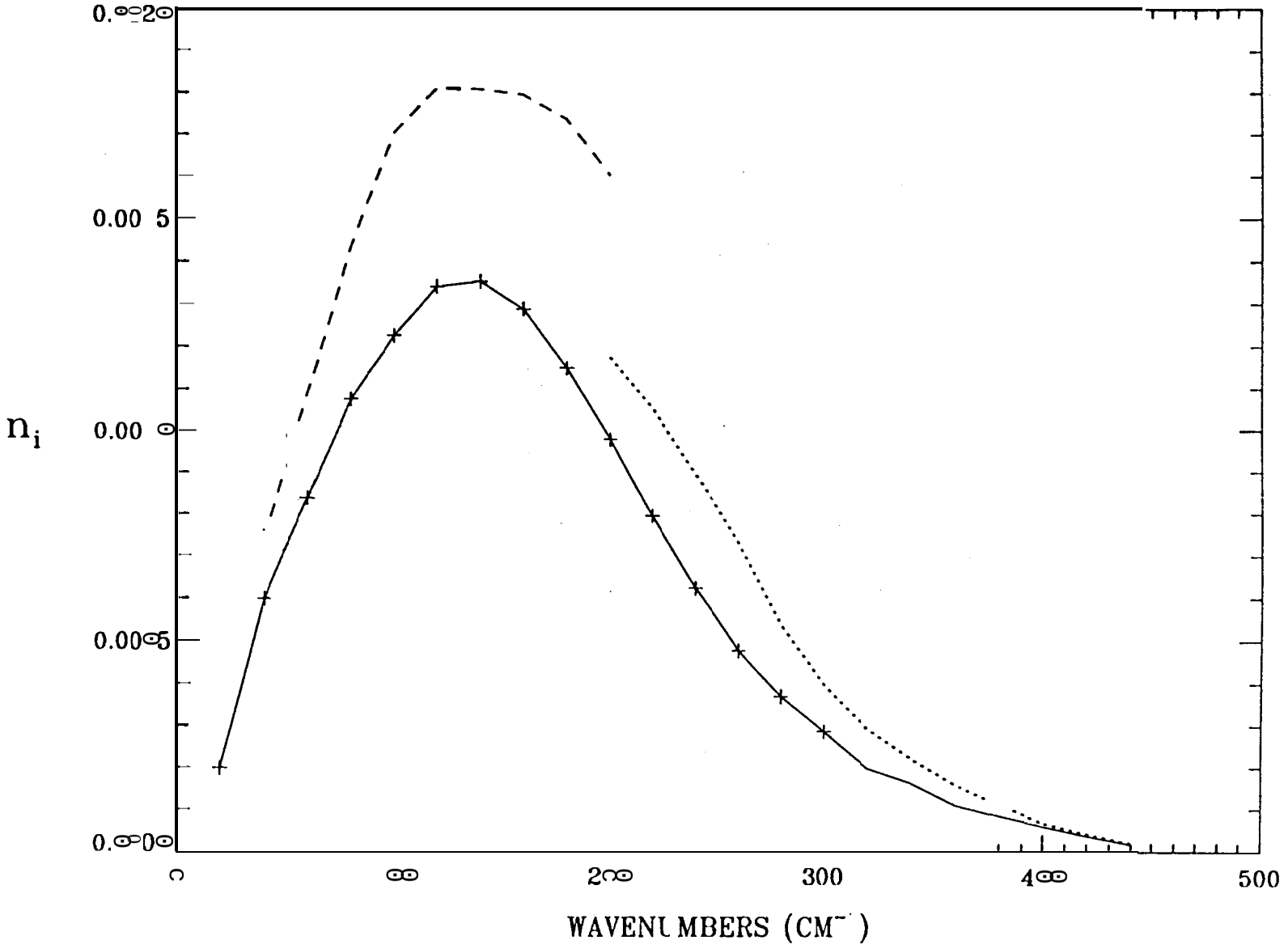
0.0020
0.00 5
0.00 0
0.0005
0.0000
n_i
0
100
200
300
400
500
WAVENUMBERS (CM⁻¹)

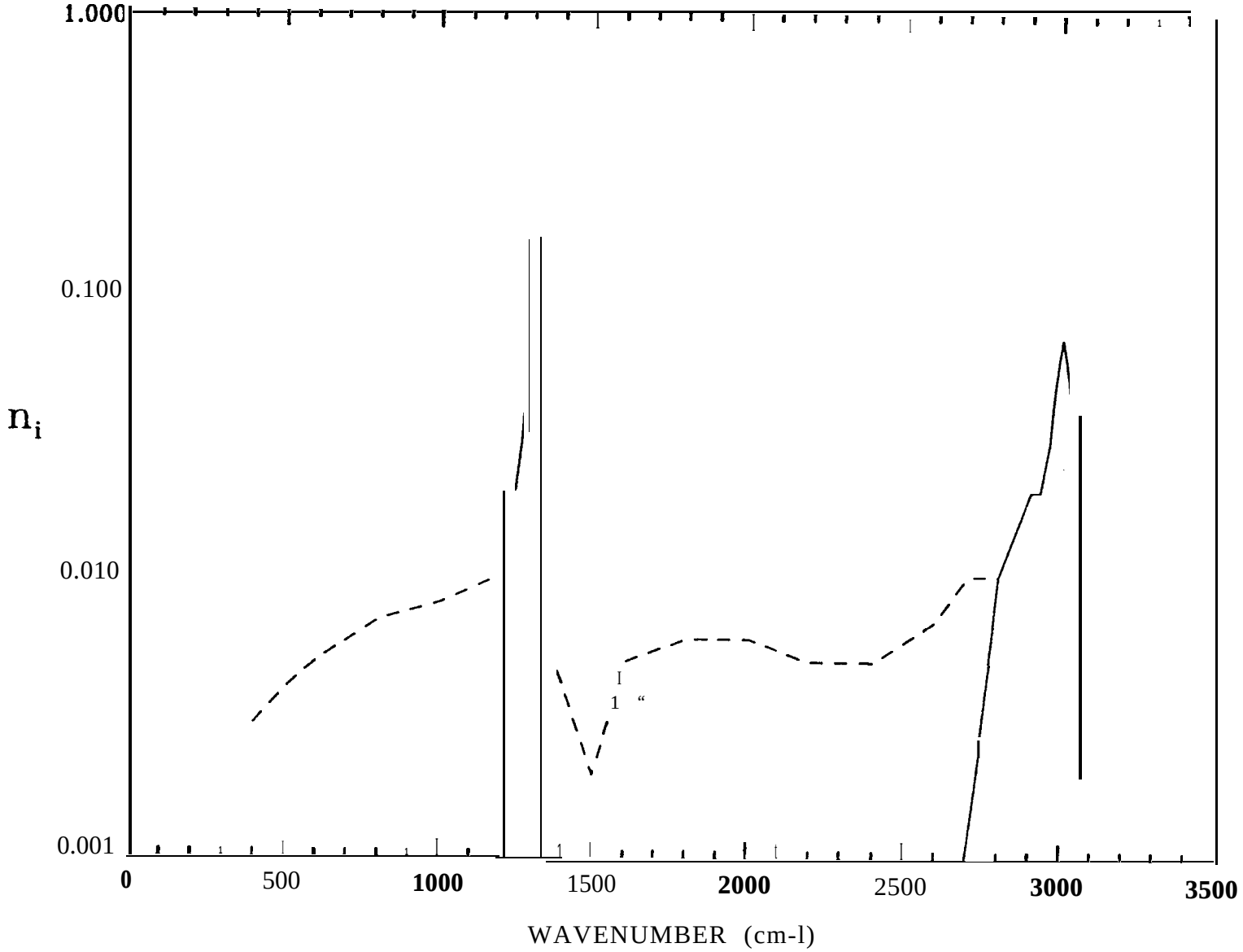
1.000
0.100
0.010
0.001
n_i
0
500
1000
1500
2000
2500
3000
3500
WAVENUMBER (cm-l)

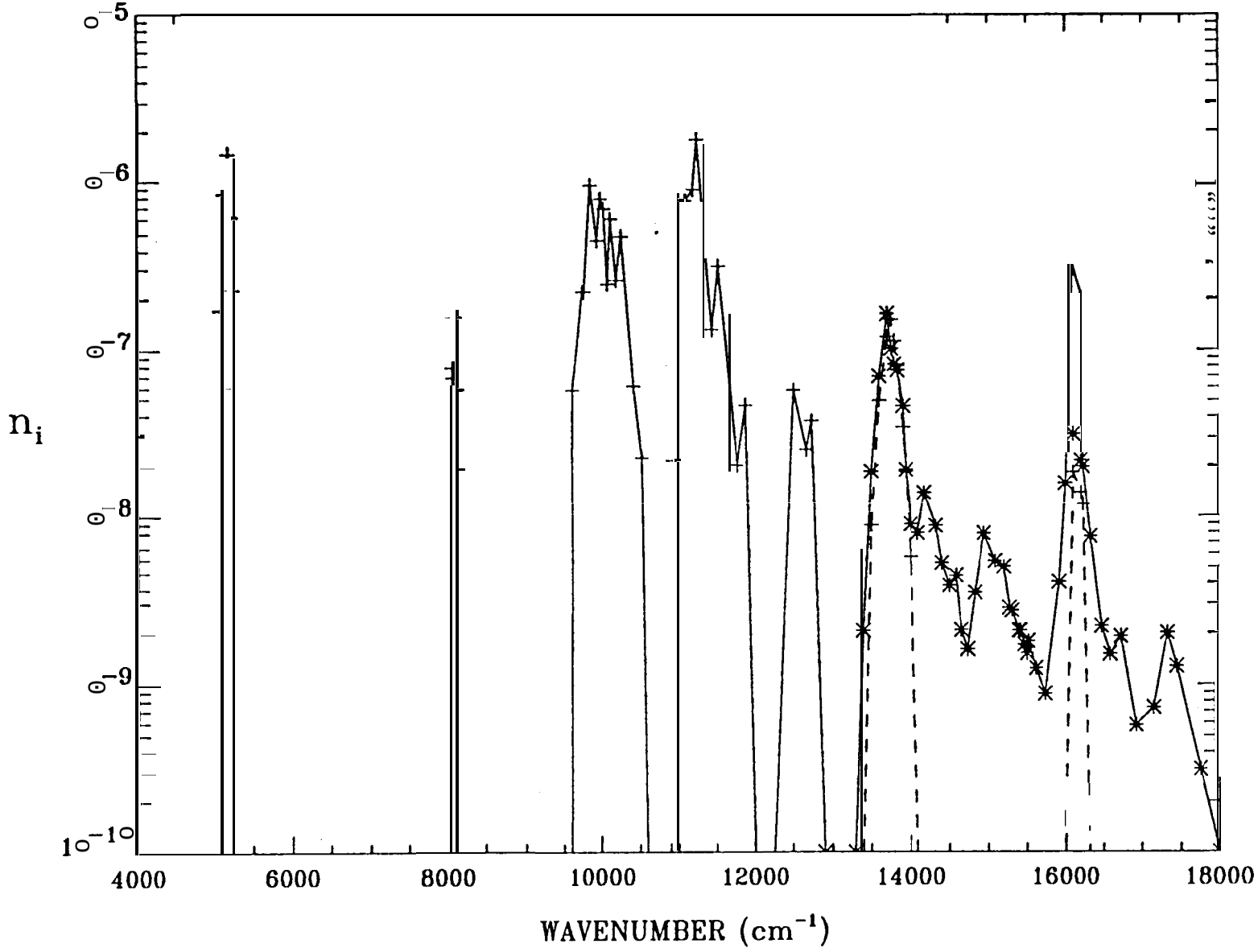
n_i
10^{-5}
10^{-6}
10^{-7}
10^{-8}
10^{-9}
10^{-10}
4000
6000
8000
10000
12000
14000
16000
18000
WAVENUMBER (cm^{-1})

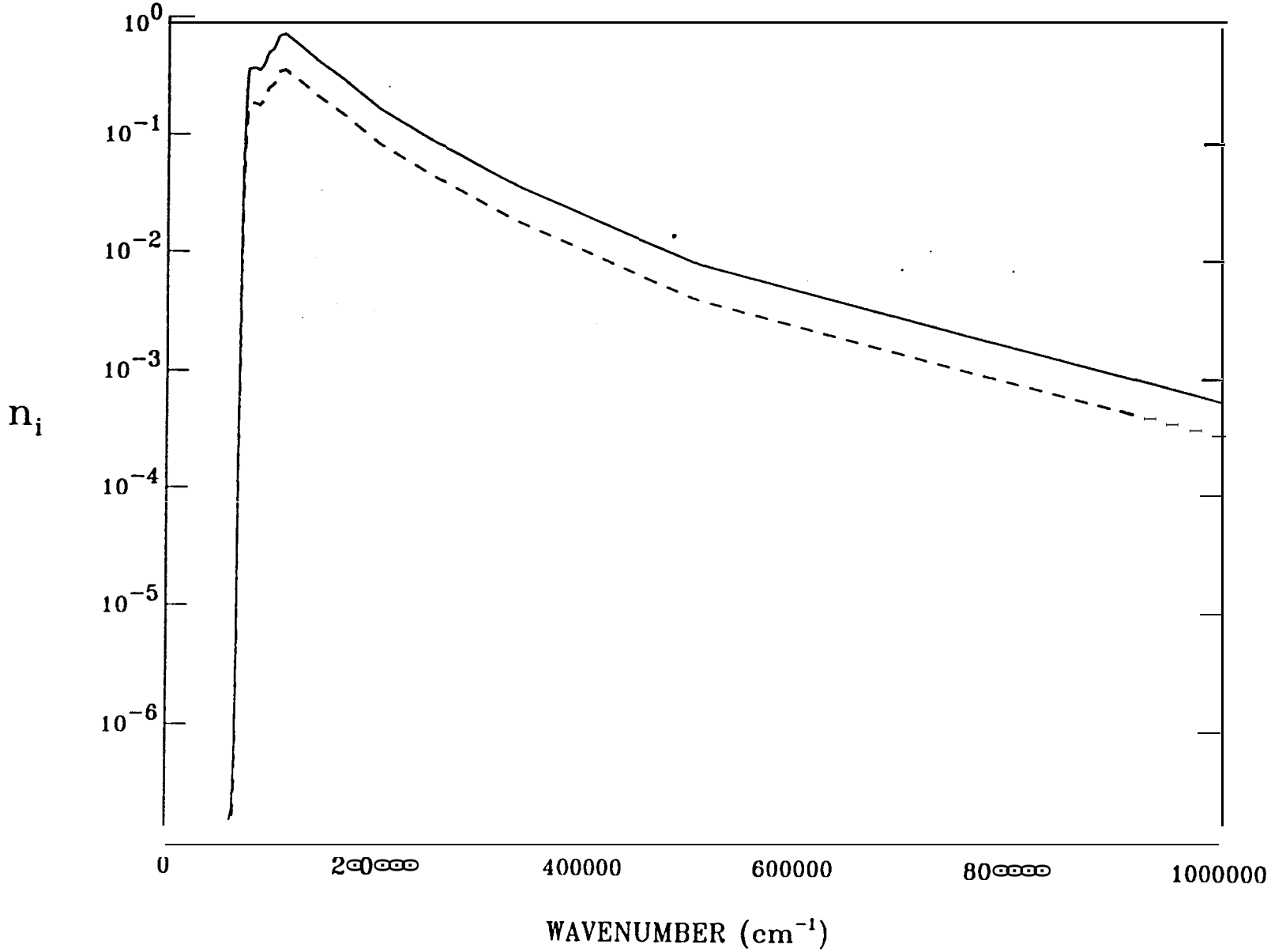
10^0
10^{-1}
10^{-2}
10^{-3}
10^{-4}
10^{-5}
10^{-6}
n_i
0
200000
400000
600000
800000
1000000
WAVENUMBER (cm^{-1})

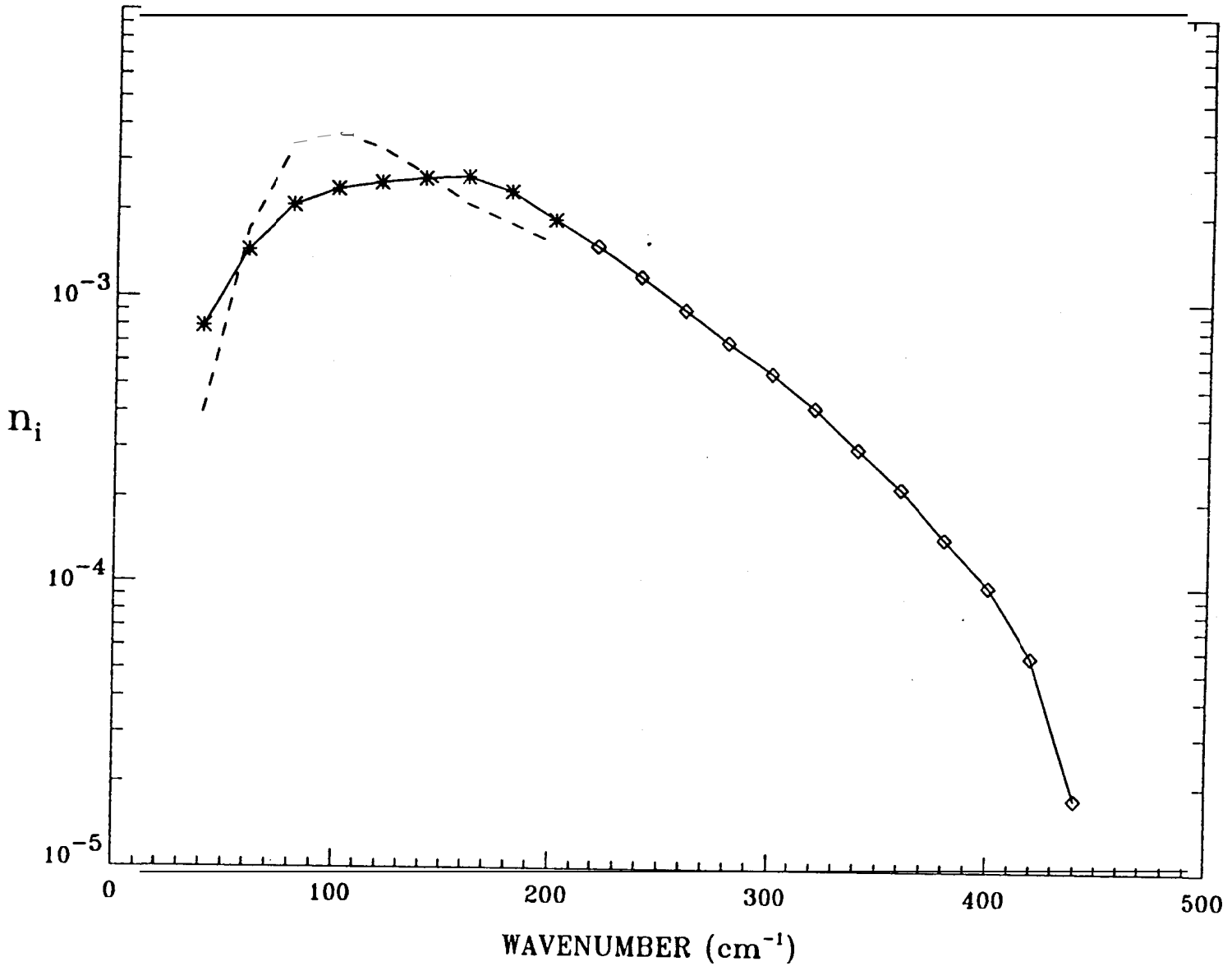
10^{-3}
10^{-4}
10^{-5}
n_i
0
100
200
300
400
500
WAVENUMBER (cm^{-1})

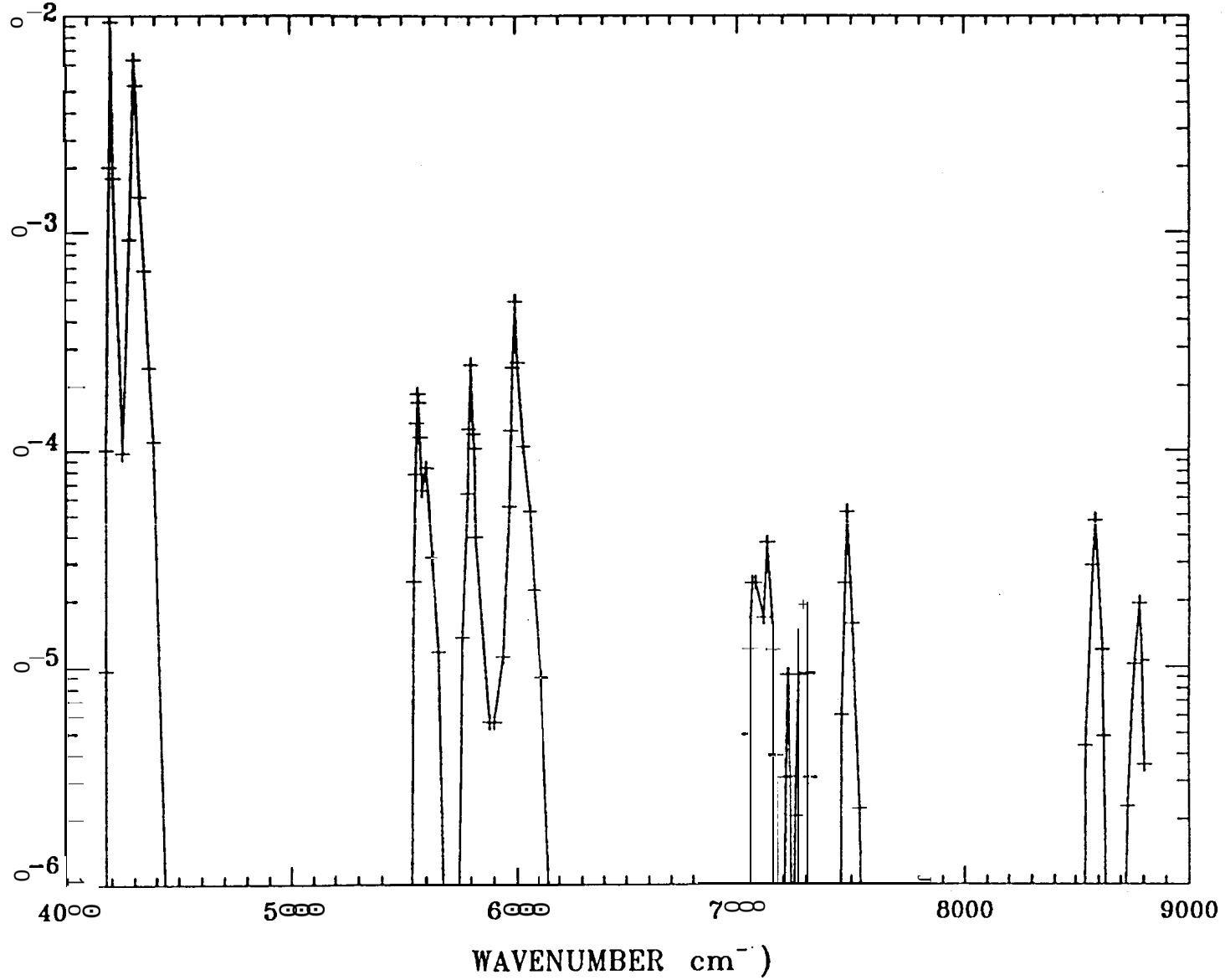
n
0
−2
−3
−4
−5
−6
4000
5000
6000
7000
8000
9000
WAVENUMBER cm⁻¹)

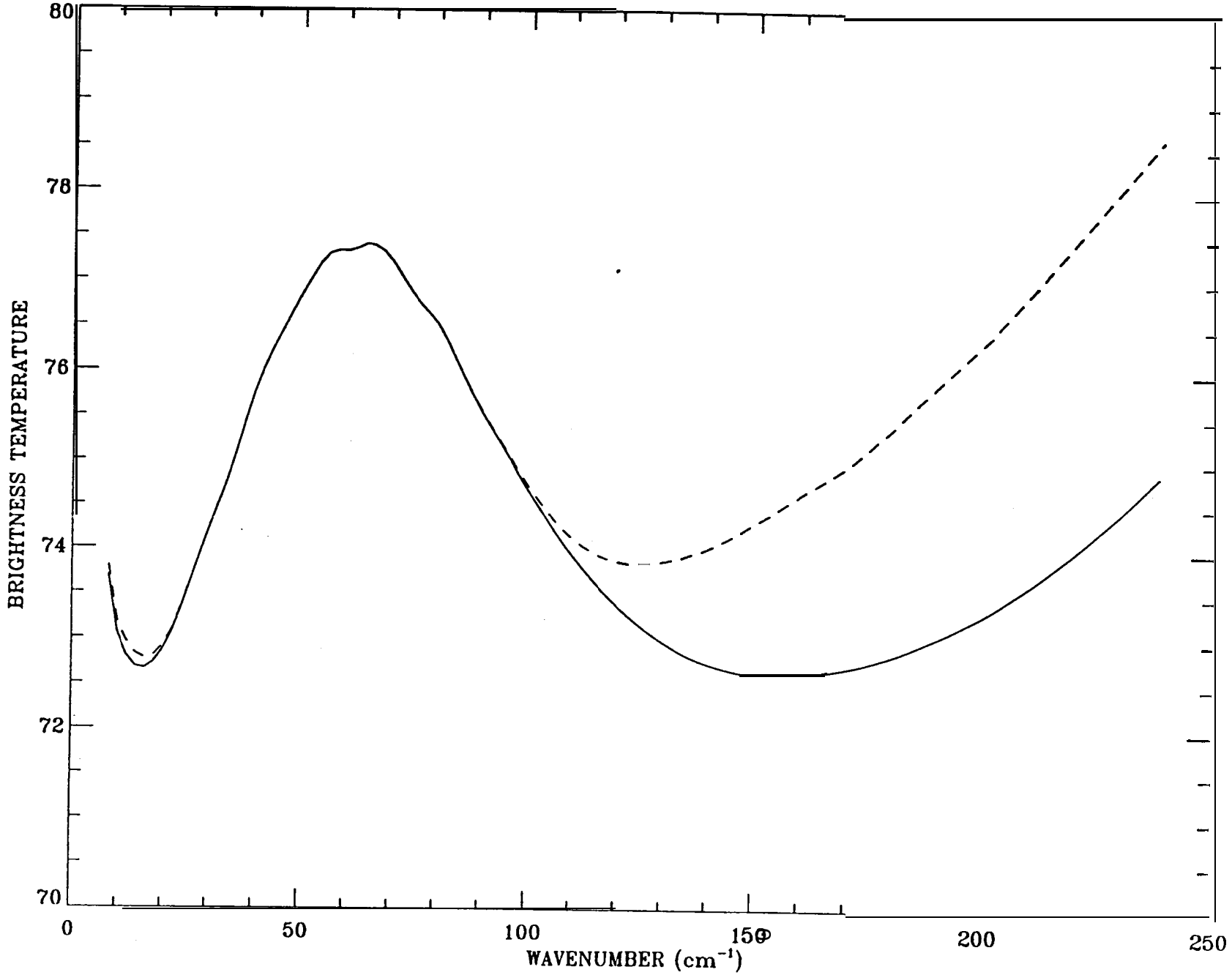
80
78
76
74
72
70
BRIGHTNESS TEMPERATURE
0
50
100
150
200
250
WAVENUMBER (cm^{-1})

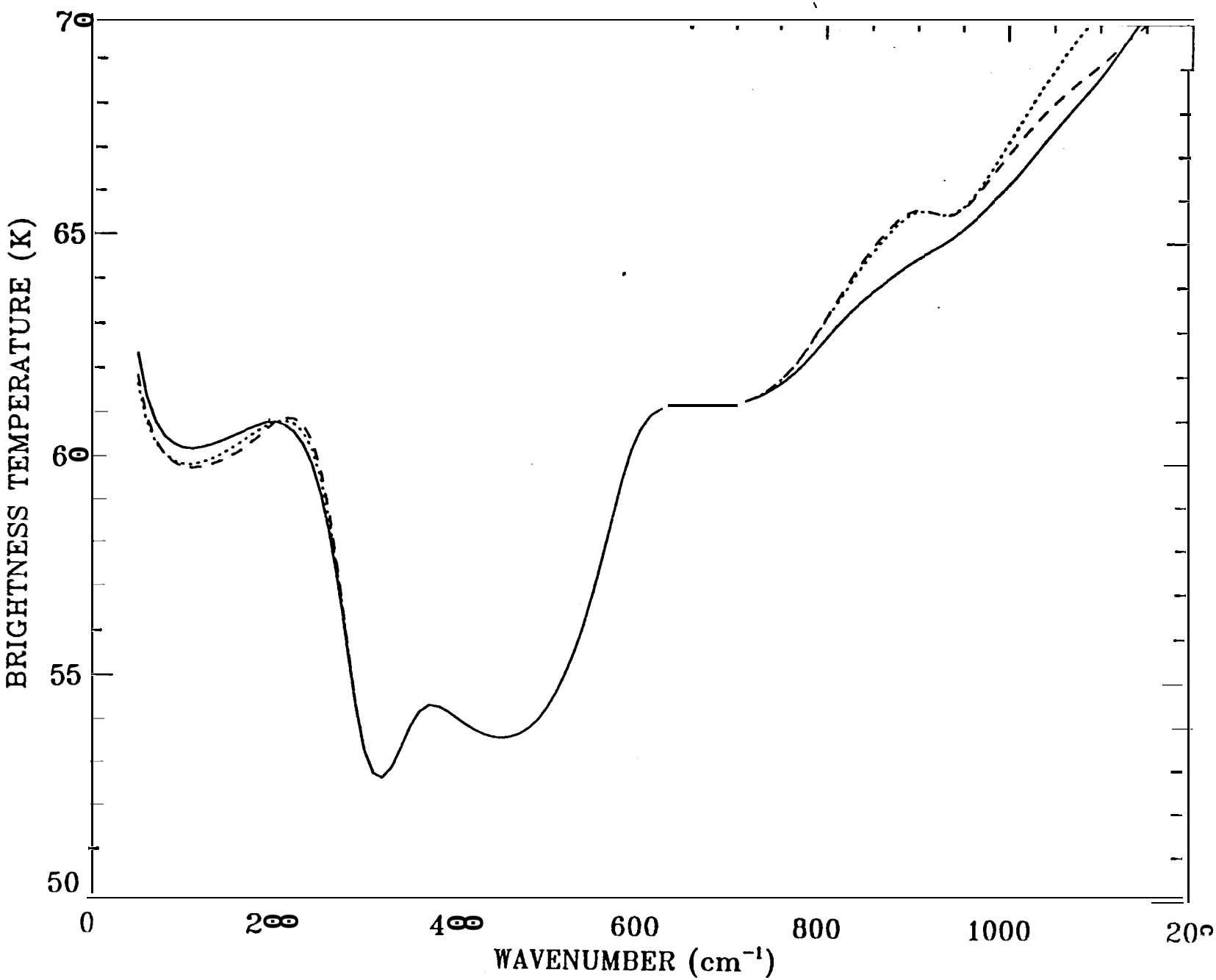
70
65
60
55
50
BRIGHTNESS TEMPERATURE (K)
0
200
400
600
800
1000
WAVENUMBER (cm^{-1})